

See discussions, stats, and author profiles for this publication at: <https://www.researchgate.net/publication/231273723>

# Catalytic Transformation of Ethylbenzene over Y-Zeolite-based Catalysts

ARTICLE *in* ENERGY & FUELS · OCTOBER 2008

Impact Factor: 2.79 · DOI: 10.1021/ef8005542

---

CITATIONS

8

---

READS

27

## 1 AUTHOR:



[Sulaiman al-khattaf](#)

King Fahd University of Petroleum and Min...

117 PUBLICATIONS 1,118 CITATIONS

SEE PROFILE

# Catalytic Transformation of Ethylbenzene over Y-Zeolite-based Catalysts

Sulaiman Al-Khattaf\*

KAUST Center in Development, King Fahd University of Petroleum & Minerals Dhahran 31261, Saudi Arabia

Received July 12, 2008. Revised Manuscript Received September 5, 2008

Catalytic transformation of ethylbenzene (EB) has been investigated over ultrastable Y (USY)-zeolite-based catalysts in a novel riser simulator at different operating conditions. The effect of reaction conditions on EB conversion is reported. The USY catalyst (FCC-Y) was modified by steaming to form a significantly lower acidity catalyst (FCC-SY). The current study shows that the FCC-SY catalyst favors EB disproportionation more than cracking. A comparison has been made between the results of EB conversion over the lowly acidic catalyst (FCC-SY) and the highly acidic catalyst (FCC-Y) under identical conditions. It was observed that increase in catalyst acidity favored cracking of EB at the expense of disproportionation. Kinetic parameters for EB disappearance during disproportionation reaction over the FCC-SY catalyst were calculated using the catalyst activity decay function based on time on stream (TOS).

## 1. Introduction

The catalytic disproportionation of ethylbenzene (EB) over zeolite-based catalyst to produce isomers of diethylbenzene (DEB) among other products has gained tremendous attention in recent years. This is due to the wide range of application of these compounds in a variety of industrial processes. For example, *para*-DEB, which is the most important of the three DEB isomers, is an important desorbent in adsorptive separation processes such as UOP Para-ex, used for the separation of xylene isomers. Also, it can be used as an intermediate in the production of *p*-divinylbenzene. Finally, it is an important monomer for the production of copolymers, such as ion-exchange resin and viscosity modifiers of lubricant oil.<sup>1</sup>

Ethylbenzene disproportionation was initially studied by Karge et al.<sup>2,3</sup> to characterize zeolites in their acid form. The selectivity of *para*-DEB in the product was generally poor. On the other hand, when medium micropore zeolites were used, significant *para*-DEB selectivity was observed. Following this pioneer work, numerous studies of the reaction were carried out over USY, Beta, MCM-22, and ZSM-5.<sup>4–6</sup> In most cases, the composition of the different DEB isomers in the reaction product was limited by thermodynamics leading to an equilibrium composition with a relatively lower amount of the *para*-isomer compared to the *meta*-isomer. This led researchers to the conclusion that the mechanism of zeolite-catalyzed EB disproportionation is the same as that of toluene disproportion-

ation, that is, shape-selectivity for the diffusion difference among *para*-, *meta*-, and *ortho*-DEB plays an important role.<sup>7</sup>

Since *para*-DEB is the most important of the three isomers, many research groups have reported efforts to improve its selectivity during EB disproportionation. Velasco et al.<sup>8</sup> studied the effect of aluminum content and crystal size on the selectivity for *para*-DEB during EB disproportionation on a ZSM-5 MFI zeolite. Their results showed that up to 90% *para*-DEB selectivity can be achieved with MFI samples having high aluminum contents and crystal size of at least 40  $\mu\text{m}$ . Park and Rhee<sup>9</sup> have also investigated EB disproportionation using a sample of MCM-22 and its dealuminated form at low temperatures. *Para*-selectivity of MCM-22 was found to increase with the degree of dealumination. Camiloti et al.,<sup>10</sup> evaluated the catalytic behavior of  $\beta$  zeolites with Si/Al ratios ranging from 18 to 33 for disproportionation of EB. It was observed that beta zeolites samples with greater Si/Al ratios have higher acid strength and showed a higher EB disproportionation. These results indicate that as the aluminum content in zeolite  $\beta$  is reduced, the strength of the associated acid sites increases.

Unlike the study of catalyst development, not much has been reported in regard to the mechanistic and kinetic studies of EB disproportionation in the open literature. A very important mechanistic investigation of the reaction by Arsenova et al.<sup>11</sup> over ZSM-5 showed that the reaction scheme follows a consecutive path. These workers reported that the first step in EB disproportionation occurs in the interior of the zeolite crystal without diffusion limitations, yielding essentially *para*-DEB as a primary product. The latter is then converted in a secondary

\* Corresponding author. Phone: +966-3-860-1429; fax: +966-3- 860-4234; E-mail: skhattaf@kfupm.edu.sa.

(1) Zhirong, Z.; Qingling, C.; Zaiku, X.; Weimin, Y.; Dejin, K.; Can, L. *J. Mol. Catal. A* **2006**, 248, 152.

(2) Karge, H. G.; Ladebeck, J.; Sarbak, Z.; Hatada, K. *Zeolites* **1982**, 2, 94.

(3) Karge, H. G.; Hatada, K.; Zheng, Y.; Fiedorow, R. *Zeolites* **1983**, 3, 13.

(4) Wang, I.; Tsai, T. C.; Aye, C. L. *Stud. Surf. Sci. Catal.* **1993**, 75, 1673.

(5) Karge, H. G.; Ladebeck, J.; Sarbak, Z.; Hatada, K. *Zeolites* **1982**, 2, 94.

(6) Tsai, T. C., Ph.D. Dissertation; National Tsing Hua University: Hsinchu, Taiwan, 1991.

(7) Keating, W. W. *J. Catal.* **1985**, 95, 512.

(8) Velasco, N. D.; Machado, M. S.; Cardoso, D.; Braz, J. *Chem. Eng* **1998**, 15, 2.

(9) Park, Se-Ho; Rhee, Hyun-Ku *Appl. Catal., A* **2001**, 219, 99.

(10) Camiloti, A. M.; Jahn, S. L.; Velasco, N. D.; Moura, L. F.; Cardoso, D. *Appl. Catal., A* **1999**, 182 (1), 107.

(11) Arsenova, N.; Haag, W. O.; Karge, H. G. In *Proceedings of the 11th International Zeolite Conference: Progress in Zeolites and Microporous Materials*, Seoul, Korea, August 12–17, 1996; Chon, H., Ihm, S. K., Uh, Y. S. Eds.; Elsevier: Amsterdam, 1997. *Stud. Surf. Sci. Catal.* Vol 105, p 1293.

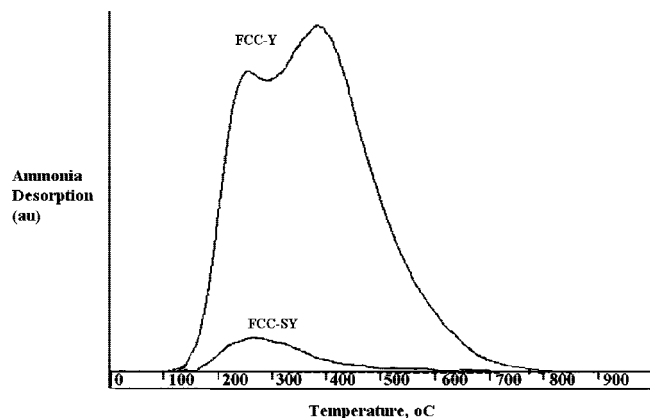


**Figure 1.** Temperature program desorption of ammonia over both catalysts.

**Table 1.** Characterization of Catalyst

catalyst	acidity (mmol/g)	BET surface area (m <sup>2</sup> /g)	crystallite size (μm)	unit cell size (Å)	Na <sub>2</sub> O wt %
FCC-SY	0.033	155	0.9	24.27	negligible
FCC-Y	0.55	190	0.9	24.50	negligible

isomerization reaction mainly to *meta*-DEB. Catalytic and sorption studies carried out by Arsenova-Hartel<sup>12</sup> would suggest that the formation of *ortho*-DEB within the pores of ZSM-5 at low temperatures (less than 522 K) is almost impossible. Arsenova-Hartel et al.,<sup>13</sup> studied the relationship between the reaction kinetics of the disproportionation of EB and the pore structure of the zeolite catalyst. Earlier studies of the kinetics revealed that over large-pore zeolites at low temperatures the reaction rate is significantly but reversibly retarded by the product DEB. In contrast, with medium-pore zeolites no product inhibition was observed. As a possible explanation, it was suggested that the difference between the adsorption constant of the inhibiting product and that of the feed is more strongly pronounced in large- than in medium-pore zeolites. The results indicate a stronger accumulation of the DEB in faujasite than in H-ZSM-5. Sorption measurements with pure EB and DEB on H-ZSM-5 and Y-zeolites confirmed the assumption that with decreasing pore-size the product is no longer sorbed more strongly in the zeolite than the feed.

Pai et al.<sup>14</sup> carried out a kinetic study of EB disproportionation in a mixture of xylene over modified HZSM-5 at temperatures of 573, 583, and 598 K. On the basis of a simple first-order model similar to the one proposed by Nayak and Rieker,<sup>15</sup> they were able to estimate the activation energy of the disproportionation reaction to be around 26.27 kJ/mol.

Recently, Tsai et al.<sup>16</sup> reported that EB can transform via three mechanisms: disproportionation (into benzene and DEB), dealkylation (into benzene and gases), and reforming to xylene. It was reported that although reforming requires dual functions (metal and acidic), disproportionation and dealkylation need only acid sites. Therefore, the yield of xylenes was increased by inactivating the external acid sites that are used for disproportionation and cracking reactions.

Despite that most of the recent work on EB disproportionation involves some modification of ZSM-5, some researchers also used pillared clays<sup>17</sup> and Al-PO<sub>4</sub>-5<sup>18</sup> for EB disproportionation.

In view of the foregoing literature, it is important to mention that most of the studies were conducted in fixed-bed reactors. Moreover, most of these studies last for several hours, where it has been proposed that EB conversion begins with an induction period (1–3 h) in which the conversion increases until a steady state is reached. The aim of this study is to investigate the catalytic transformation of EB over Y-zeolite in a fluidized-bed reactor in a short contact time (3–15 s). Two forms of the catalyst will be used: a highly acidic FCC-Y and a lowly acidic FCC-SY. The study will focus on the effect of reaction conditions (time, temperature, and conversion) and catalyst acidity on the conversion of EB, the cracking-to-disproportionation (C/D) ratio, distribution of DEB (DEB) isomers, and benzene/DEBs (B/DEB) ratio. An attempt will also be made to model EB disproportionation over FCC-SY catalyst, and the kinetic modeling results will be compared with the experimental data.

## 2. Experimental Procedure

**2.1. The Riser Simulator.** All the experimental runs were carried out in the Riser Simulator. This reactor is novel bench scale equipment with an internal recycle unit invented by de Lasa.<sup>19</sup> The Riser Simulator consists of two outer shells, the lower section and the upper section, which allow easy loading or unloading of the catalyst. The reactor was designed in such way that an annular space is created between the outer portion of the basket and the inner part of the reactor shell. A metallic gasket seals the two chambers with an impeller located in the upper section. A packing gland assembly and a cooling jacket surrounding the shaft provide support for the impeller. Upon rotation of the shaft, gas is forced outward from the center of the impeller toward the walls. This creates a lower pressure in the center region of the impeller, thus inducing flow of gas upward through the catalyst chamber from the bottom of the reactor annular region, where the pressure is slightly higher. The impeller provides a fluidized bed of catalyst particles as well as intense gas mixing inside the reactor. A detailed description of various Riser Simulator components, sequence of injection, and sampling can be found in ref 20.

**2.2. Materials.** Ultrapure Y-zeolite (USY) was obtained from Tosoh Company. The Na-zeolite was ion exchanged with NH<sub>4</sub>NO<sub>3</sub> to replace the sodium cation with NH<sub>4</sub><sup>+</sup>. Following this, NH<sub>3</sub> was removed and the H form of the zeolite was spray-dried using kaolin as the filler and silica sol as the binder. The resulting 60 μm catalyst particles had the following composition: 30 wt % zeolite, 50 wt % kaolin, and 20 wt % silica sol. The process of sodium removal was repeated for the palletized catalyst. Following this, the catalyst was calcined for 2 h at 600 °C, forming catalyst FCC-Y. Finally, half of FCC-Y catalyst particles (60 μm average size) were treated with 100% steam at 760 °C for 5 h to produce FCC-SY catalyst. It has to be mentioned here that the catalyst matrix (kaolin) is inactive and all the activity is due to the zeolite.

Analytical grade (99% purity) pure Ethylbenzene was obtained from Sigma-Aldrich. All chemicals were used as received and no attempt was made to further purify the samples.

**2.3. Procedure.** Regarding the experimental procedure in the Riser Simulator, 0.81 g of catalyst was loaded into the Riser

(12) Arsenova-Hartel, N.; Bludau, H.; Schumacher, R.; Haag, W. O.; Karge, H. G.; Brunner, E.; Wild, U. *Catal* **2000**, *191*, 326–331.

(13) Arsenova-Hartel, N.; Bludau, H.; Haag, W. O.; Karge, H. G. *Microporous Mesoporous Mater.* **2000a**, *35*–6, 113–119.

(14) Pai, S. M.; Sharanappa, N.; Anilkumar, M.; Kadam, S. T.; Bokade, V. V. *Chem. Eng. Res. Des.* **2004**, *82* (A10), 1391–1396.

(15) Nayak, V. S.; Rieker, L. *Appl. Catal., A* **1986**, *23*, 403–411.

(16) Tsai, T. C.; Wang, I.; Huang, C.; Liu, S. *Appl. Catal., A* **2007**, *321*, 125–134.

(17) Jeronimo, D.; Guil, J. M.; Corbella, B. M.; Vasques, H.; Miranda, A.; Silva, J.; Lobato, A.; Pires, J.; Carvalho, A. *Appl. Catal., A* **2007**, *330*, 89–95.

(18) Raj, K.; Meenakshi, M.; Vijayaraghavan, V. *J. Molec. Cata.* **2007**, *270*, 195–200.

(19) de Lasa, H. T. US Patent 5102628, 1992.

(20) Kraemer, D. W. Ph.D. Dissertation; University of Western Ont.: London, Canada, 1991.

**Table 2. Product Distribution (wt %) at Various Reaction Conditions for Toluene FCC-SY**

time (s)	conv. (%)	gas	benzene	toluene	<i>m</i> -DEB	<i>p</i> -DEB	<i>o</i> -DEB	other	total DEB	% DEB
400 °C										
3	1.00		0.50		0.20	0.10	0.04	0.03	0.34	34.00
5	2.30		1.22		0.53	0.26	0.07	0.20	0.86	37.48
7	3.00		1.58		0.72	0.36	0.10	0.24	1.19	39.56
10	4.23		2.12	0.05	1.02	0.55	0.15	0.25	1.73	40.84
13	4.92		2.44	0.06	1.31	0.66	0.17	0.28	2.14	43.50
15	5.27		2.57	0.06	1.44	0.71	0.20	0.29	2.36	44.72
450 °C										
3	1.42		0.85		0.29	0.14		0.14	0.44	30.68
5	2.40		1.31		0.58	0.28	0.09	0.13	0.94	39.10
7	3.20	0.05	1.62	0.04	0.78	0.38	0.12	0.21	1.27	39.73
10	4.83	0.10	2.38	0.07	1.23	0.60	0.18	0.28	2.01	41.63
13	6.20	0.19	3.02	0.09	1.59	0.77	0.24	0.30	2.60	42.00
15	7.50	0.23	3.49	0.10	1.88	0.91	0.27	0.54	3.06	40.80
500 °C										
3	2.84	0.17	1.56	0.08	0.46	0.22	0.08	0.27	0.76	26.77
5	4.80	0.36	2.40	0.13	0.77	0.37	0.13	0.60	1.27	26.38
7	5.55	0.42	2.88	0.15	0.98	0.46	0.16	0.43	1.60	28.89
10	7.32	0.54	3.77	0.21	1.35	0.65	0.22	0.50	2.22	30.32
13	9.80	0.87	4.99	0.32	1.66	0.79	0.28	0.75	2.73	27.91
15	12.45	1.03	6.25	0.36	2.23	1.07	0.37	1.02	3.66	29.41

Simulator basket. The system was then sealed and tested for any pressure leaks. Then, the reactor was heated to the desired reaction temperature. The vacuum box was also heated to around 250 °C and evacuated to around 0.5 atm to prevent any condensation of hydrocarbons inside the box. The heating of the Riser Simulator was conducted under continuous flow of argon (inert gas). The catalyst was activated for 15 min at 620 °C in a stream of air. The temperature controller was set to the desired reaction temperature, in the same manner the timer was adjusted to the desired reaction time. At this point the gas chromatograph was started and set to the desired conditions.

Once the reactor and the gas chromatograph reached the desired operating conditions, the ethyl benzene was injected directly into the reactor via a loaded syringe. After the reaction, the four-port valve immediately opened, ensuring that the reaction was terminated and that the entire product stream was sent to the gas chromatograph via a preheated vacuum box chamber. The products were analyzed in an Agilent 6890N gas chromatograph with a flame ionization

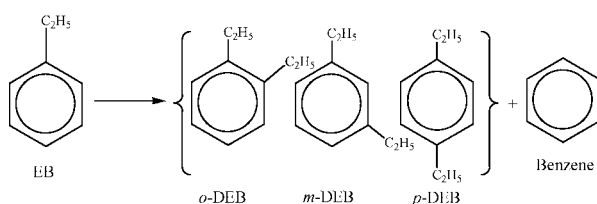
detector (FID) and a capillary column INNOWAX, 60 m cross-linked methyl silicone with an internal diameter of 0.32 mm.

The injection of the reactant was carried out at atmospheric pressure. Subsequently, the pressure increases upon reactant vaporization. The reaction pressure of the system after reactant vaporization was about 2.0–2.5 atm. However, the reaction was carried out at constant pressure.

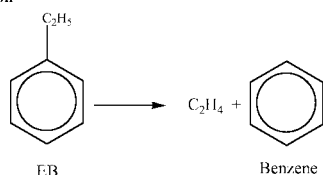
### 3. Results and Discussion

Catalytic experiments were carried out in the Riser Simulator at a catalyst/reactant ratio of 5 (mass of catalyst = 0.81 g, mass

#### Disproportionation Reaction



#### Cracking Reaction



#### Transalkylation Reaction

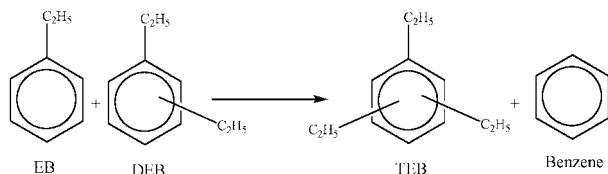


**Figure 2.** Some probable reactions that can take place during EB disproportionation.

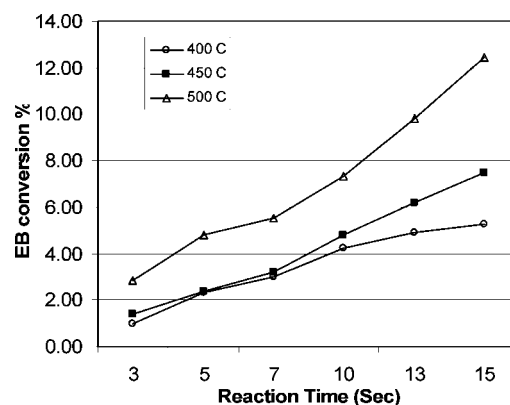


**Figure 3.** Conversion of EB with respect to reaction time and temperature using FCC-SY catalyst.

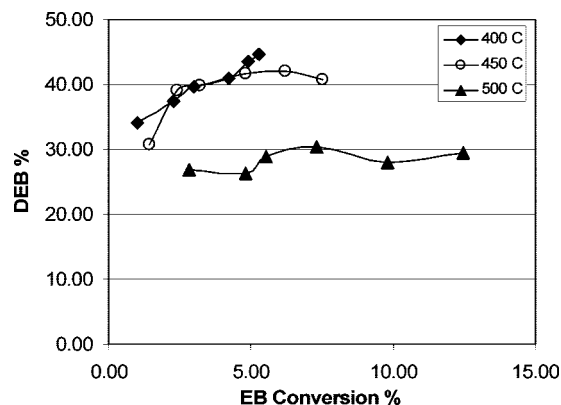


**Figure 4.** Selectivity of DEB with respect to EB conversion and reaction temperature using FCC-SY catalyst.

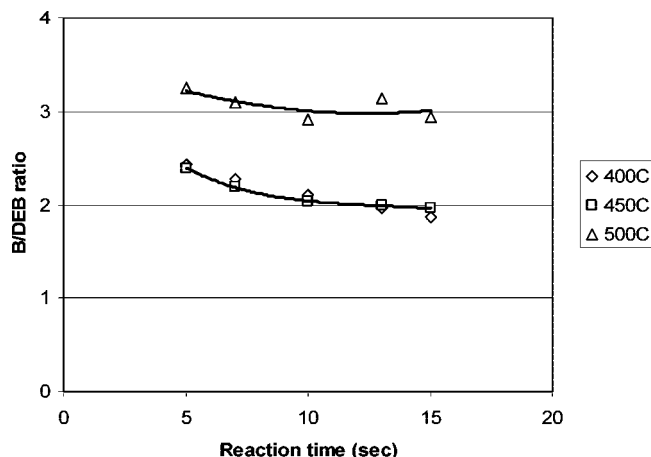


Figure 5. Molar ratio of benzene/DEB with respect to reaction time and temperature using FCC-SY catalyst.

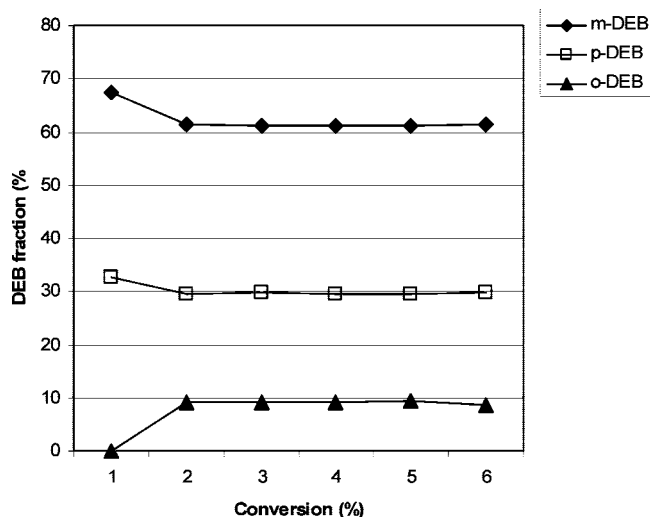


Figure 6. DEB isomers distribution over FCC-SY catalyst at 400 °C.

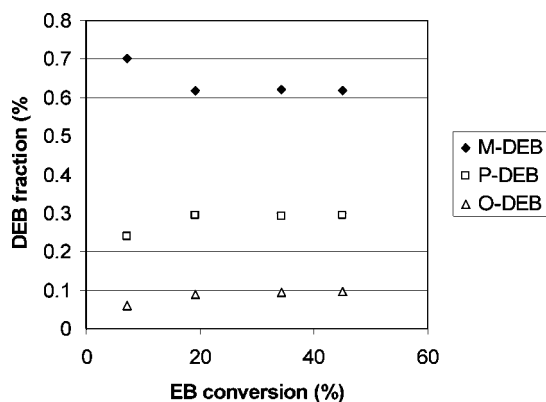


Figure 7. DEB isomers distribution over FCC-Y catalyst at 400 °C.

of reactant injected = 0.162 g; residence times of 3, 5, 7, 10, 13 and 15 s; and temperatures of 400, 450, and 500 °C. During the course of the investigation, a number of runs were repeated to check for reproducibility in the conversion results, which was found to be excellent. Typical errors were in the range of  $\pm 2\%$ .

**3.1. Catalyst Characterization.** The BET surface area was measured according to the standard procedure ASTM D-3663, using a NOVA 1200 unit (Quanta Chrome). The acid property of the catalyst was characterized by  $\text{NH}_3$  temperature-programmed desorption ( $\text{NH}_3$ -TPD). In all the experiments, 50 mg of sample was outgassed at 400 °C for 30 min in flowing

helium and then cooled down to 150 °C. At that temperature,  $\text{NH}_3$  was adsorbed on the sample by injecting pulses of 2  $\mu\text{L}$ /pulse. The injection was repeated until the amount of  $\text{NH}_3$  detected was the same for the last two injections. After the adsorption of  $\text{NH}_3$  reached saturation, the sample was flushed at 150 °C for 1 h with He to remove excess  $\text{NH}_3$ , and then the temperature was programmed at 30 °C/min up to 1000 °C in flowing He at 30 mL/min (see Figure 1). The flame ionization detector was used to monitor the desorbed  $\text{NH}_3$ . The results of the catalyst characterization are summarized in Table 1.

**3.2. Ethylbenzene Transformation Reactions using FCC-SY Catalyst.** The results of EB transformation over FCC-SY catalysts at different reaction temperatures and contact times are presented in Table 2. It was observed that EB conversion increases with both reaction time and temperature. The experimental results showed that disproportionation, cracking, and transalkylation reactions are simultaneously taking place. Some of the probable reactions that can take place during disproportionation of EB are presented in Figure 2. The disproportionation reaction results in the formation of benzene and DEB isomers (*m*-DEB, *p*-DEB, and *o*-DEB). The DEB produced during disproportionation of EB can further react with the EB to form a transalkylation product; triethylbenzene (TEB). It has been observed (Table 2 and Figure 3) that conversion of EB increases with increase in temperature as well as reaction time. The selectivity of DEB with respect to temperature and conversion of EB has been presented in Figure 4. It can be seen that the EB conversion has no significant effect on DEB selectivity. However, DEB selectivity is essentially influenced by the temperature of the reaction. The DEB selectivity is almost constant at 500 °C with a maximum value of 30%. The decrease in selectivity of DEB at high temperature, shown in Figure 4, suggests the increasing role of other reactions such as cracking and transalkylation at higher temperatures. Pai et al.<sup>14</sup> and Das et al.<sup>21</sup> reported similar behavior for DEB selectivity with temperature. They reported that as reaction temperature increases, EB conversion and benzene selectivity increase while DEB selectivity decreases.

It has been observed (Table 2) that the compositional distribution of DEB isomers *m*-DEB/*p*-DEB/*o*-DEB is approximately 6:3:1, respectively. This composition distribution is almost constant at all temperatures, indicating equilibrium values.

It was observed that gaseous product increased with the increase in reaction temperature. Although no gaseous product was detected by the GC at 400 °C, the percentage of gaseous product in the reaction product rose to between 1–3% and 5–8% at 450 and 500 °C, respectively. The increase in gaseous product with increase in reaction temperature can be explained on the basis of increase in the cracking reaction. Furthermore, it can be seen from Figure 4 that at 400 and 450 °C reaction temperatures, DEB selectivity reached a maximum and started to decrease with increasing temperature whereas according to Table 2 the gases yield (mainly ethylene) increases. This could be explained based on the DEB secondary cracking at high temperature and large contact time. The same trend over H-Y-zeolite was reported by Asrenova-Hartel et al.<sup>13</sup>

The molar ratio of benzene/DEB (B/DEB) has been plotted versus reaction temperature and reaction time in Figure 5. It has been observed that in all cases this ratio is more than unity and increases with increase in reaction temperature. This ratio indicates the significance of the ethyl group transfer. Moreover,

(21) Das, J.; Bhat, Y.; Halgeri, A. *Ind. Eng. Chem. Res.* **1993**, 32, 2525–2529.



**Table 3. Product Distribution (wt %) at Various Reaction Conditions for Toluene FCC-Y**

time (s)	conv. (%)	gas	benzene	toluene	<i>m</i> -DEB	<i>p</i> -DEB	<i>o</i> -DEB	other	total DEB	% DEB
350 °C										
3										
5	14.6	2.43	8.1	2.02	0.62	0.30	0.01	1.5	0.93	6.3
7										
10	26.7	4.6	13.6	4.6	0.96	0.46	0.02	2.4	1.44	5.4
13										
15	35.79	5.76	17.4	6.7	1.2	0.58	0.05	3.2	1.83	5.1
400 °C										
2	7.3	1.1	3.91	1.02	0.35	0.12	0.03	0.77	0.5	6.8
5	19.23	3.56	9.41	3.80	0.42	0.20	0.06	1.72	0.68	3.54
7										
10	34.39	6.35	15.74	7.37	0.72	0.34	0.11	3.65	1.16	3.38
13										
15	45.09	8.38	19.91	9.90	0.90	0.43	0.14	5.29	1.46	3.25
450 °C										
2	9.1	1.5	4.5	1.7	0.2	0.074	0	1	0.27	3
3	12.6	2.1	6.1	2.4	0.27	0.11	0	1	0.38	3
5	21.57	4.34	10.04	4.71	0.31	0.14	0.00	1.96	0.45	2.09
7										
10	36.48	7.34	16.03	8.49	0.46	0.21	0.07	3.78	0.75	2.06
13										
15	45.99	9.69	19.40	10.91	0.47	0.22	0.08	5.00	0.76	1.66
500 °C										
3	13.1	2.43	6.2	2.73	0.24	0.12	0.1	1.2	0.46	3.5
5	22.47	4.90	10.08	5.10	0.19	0.09	0.00	1.99	0.28	1.24
7										
10	37.22	8.48	15.90	8.73	0.25	0.11	0.00	3.51	0.36	0.97
13										
15	47.50	11.07	19.69	11.34	0.29	0.13	0.05	4.60	0.47	0.99

the deficit in the yield of DEB compared to that of benzene indicates the amount of EB that is converted to polyakylated

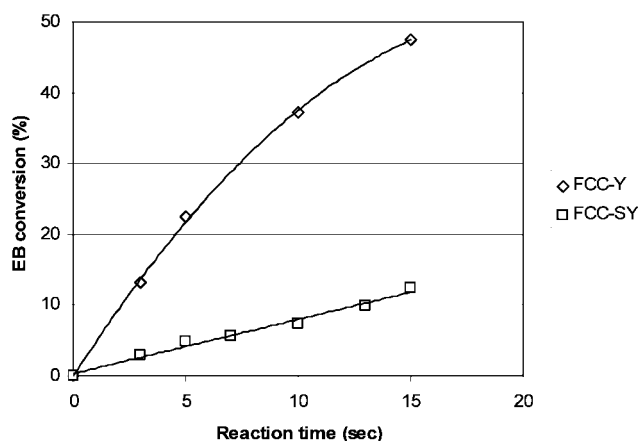


**Figure 8.** Conversion of EB with respect to reaction time for FCC-Y and FCC-SY catalysts at 500 °C.

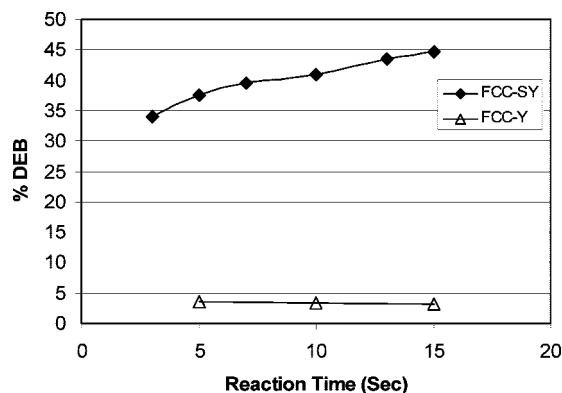


**Figure 9.** Selectivity of DEB with respect to reaction time for FCC-Y and FCC-SY catalysts at 400 °C.

**Table 4. Coke Yield (wt %) for the Two Catalysts at Various Reaction Conditions**

time (s)	coke yield (wt %) FCC-SY	coke yield (wt %) FCC-Y
350 °C		
10		1.3
15		1.6
400 °C		
5	0.06	0.94
10	0.08	1.5
15	0.1	1.8
500 °C		
5	0.03	1
10	0.033	1.7
15	0.035	2.2

**Table 5. Estimated Kinetic Parameters EB Time on Stream (TOS Model)**

parameters	values
$E_D$ (kJ/mol)	35.51
95% CL	6.38
$A_D^a \times 10^4$ (m <sup>3</sup> /kg of catalyst·s)	3.8
95% CL $\times 10^4$	0.8
$\alpha$	0.039 (0.035)

<sup>a</sup> Pre-exponential factor as in the Arrhenius equation form with  $T_0$ .

**Table 6. Correlation Matrix for Parameters**

	$k_{disp}$	$E_{disp}$	$\alpha$
$k_{disp}$	1.0000	-0.1636	0.9527
$E_{dis}$	-0.1636	1.0000	-0.0094
$\alpha$	0.9527	-0.0094	1.0000

molecules that are adsorbed in the catalyst surface.<sup>22</sup> The increase in undesirable reactions such as cracking and transalkylation of DEB with EB also lead to a higher B/DEB ratio. The cracking and transalkylation reactions result in increase in the amount of benzene and decrease in the amount of DEB, causing further increase in the B/DEB ratio.<sup>23</sup> The difference between the yields of benzene and DEB has also been reported in the literature.<sup>9</sup> It was suggested that the deficit in DEBs is due to the fact that DEB molecules are more strongly adsorbed

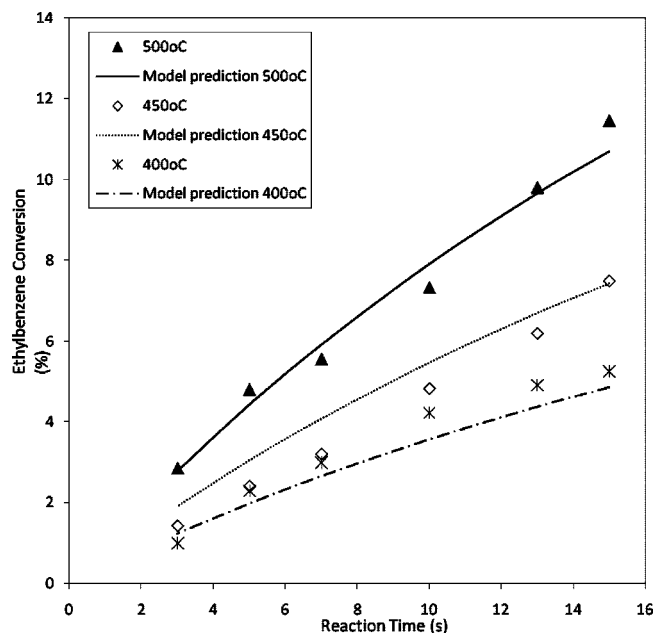


**Figure 10.** Comparison of model prediction of EB conversion with experimental data at 400, 450, and 500 °C.

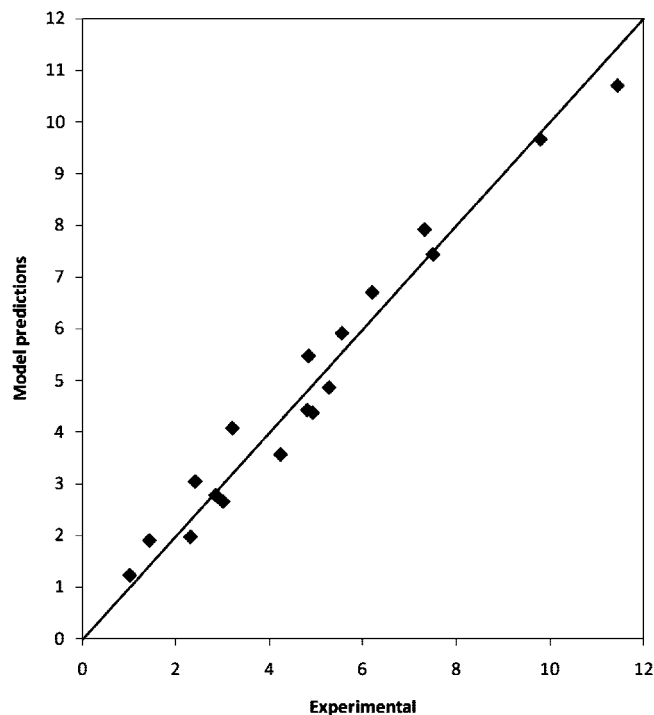


**Figure 11.** Reconciliation plot between model predictions and experimental data.

than benzene on the catalyst surface and are converted to other compounds. It can be seen in Figure 5 that temperature and reaction time (or EB conversion) have opposite effects on the B/DEB ratio. Although this ratio was found to increase with increase in temperature, it decreases with increase in reaction time. For example, for a reaction time of 15 s, this ratio was approximately 2 at 400 °C, but it increased to about 3 as temperature was increased to 500 °C. Conversely, at 400 °C reaction temperature, the B/DEB ratio was found to decrease

from approximately 2.5 to about 2 as the reaction time increased from 5 to 15 s. The observed value of the B/DEB ratio at 400 °C is not far from the value of about 1.5 reported by De Vos et al.<sup>22</sup> over a Y-zeolite-based catalyst at a temperature of 320 °C. These values are about double the values of 1.10–1.25 reported by Mishin et al.<sup>25</sup>

Figure 6 shows the distribution of DEBs isomers over FCC-SY at different conversions at a reaction temperature of 400 °C. It can be seen from this figure that all isomers are at their equilibrium composition, which does not change with the level of conversion. The equilibrium composition of *m*-DEB, *p*-DEB, and *o*-DEB at 400 °C are approximately 60, 30, and 10, respectively. Figure 7 shows that DEBs isomers distribution over FCC-Y. Even at the high acidic catalyst (FCC-Y) the isomers are at their equilibrium composition. Because Y-zeolite has large pores that can accommodate the formation of these isomers, it is believed that these isomers are primary products. These data corresponds well with the DEB equilibrium data reported in the works of Hua Chen et al. and Misin et al.<sup>24,25</sup> Moreover, according to Table 3, the *p*-DEB/*m*-DEB ratio is in the range of 0.47–0.49, which is close to the equilibrium ratio.<sup>25</sup>

### 3.4. Comparison of FCC-Y and FCC-SY Catalysts.

**3.4.1. Reactivity.** The results of the transformation reaction of EB over FCC-Y catalysts at different reaction temperatures and contact times are presented in Table 3. The conversions of EB at 500 °C over FCC-Y and FCC-SY catalysts have been plotted against reaction time in Figure 8. It has been observed that FCC-Y catalyst having high acidity (16 times that of FCC-SY) shows by far a higher activity, as reflected in much higher EB conversions compared to the FCC-SY. It is interesting to see from Figure 6 that, at a reaction temperature of 500 °C and reaction time of 15 s, the conversions over the FCC-Y and FCC-SY catalysts are approximately 47 and 7%, respectively, that is, about 7 times higher over FCC-Y than the FCC-SY catalyst. On the other hand, the effect of temperature on the conversion over FCC-Y catalyst as can be seen from Table 3 is not very significant.

**3.4.2. DEB Yield.** The selectivity of DEB over FCC-Y and FCC-SY catalysts has been plotted against reaction time in Figure 9. It can be observed from this figure that FCC-SY catalyst having low acidity exhibited very high DEB selectivity, ~45% at 400 °C for a reaction time of 15 s, whereas the corresponding value for FCC-Y is only 3%. Over both catalysts it has been noticed that DEB selectivity decreases with increase in temperature. The cracking reaction is the major reaction over FCC-Y. Consequently, a large amount of gas is observed. Toluene was found to be the second most important product after benzene for FCC-Y catalyst. Other methylbenzene products such as xylenes and trimethylbenzene were also detected in an appreciable amount, which was not the case for FCC-SY.

**3.4.3. Disproportionation-to-Cracking (D/C) Ratio.** FCC-SY consistently yielded higher disproportionation products compared to FCC-Y, as shown in Tables 2 and 3. On the other hand, FCC-Y produced more cracked products (gases and methylbenzenes) than FCC-SY. This indicates that the high acidity of FCC-Y favors the cracking reaction, whereas the low acidity favors the disproportionation reaction. Karge et al.<sup>2</sup> reported that EB conversion over zeolite is affected by zeolite acid sites. Furthermore, it was also found that the acidity strength of these sites play a major role on EB transformation.<sup>3,25</sup> It is well-known that hydrothermal removal of Al atoms from

(22) De Vos, Ernst, S. Petrego, C.; Oconnor, C.; Stocker, M. *Micro Meso Mater.* **2002**, *56*, 185–192.

(23) Arsenova, W.; Haag, H.; Karge, H.; Chon, H. s.-k. Ihm, Y. S. U. *Stud. Surf. Sci. Catal.* **1997**, *105*, 1293.

(24) Hua Chen, W.; Tsai, T.; Jong, S.; Zhao, Q.; Tsai, C.; Wang, I.; Lee, H.; Liu, S. *J. Molec. Catal. A* **2002**, *181*, 41–55.

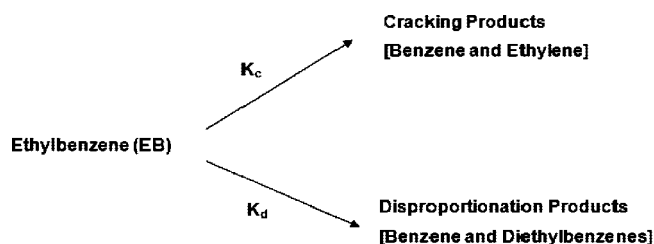
(25) Mishin, I.; Beyer, H.; Karge, H. *Appl. Catal., A* **1999**, *180*, 207.

Y-zeolite framework increases the strength of their acid sites and creates a secondary pore system.<sup>27,28</sup> Removal of the Al framework by steaming decreases acidity, but the fraction of the isolated (0-NNN) Al atoms increases, resulting in an increase in the acid strength of the active sites.<sup>27,28</sup> FCC-SY has more 0-NNN sites than FCC-Y, which explains the higher disproportionation activity for FCC-SY compared to FCC-Y. Table 1 reports the unit cell size for FCC-Y and FCC-SY to be 24.5 and 24.27 Å, respectively. On the basis of these unit cell sizes, 0-NNN sites percentage can be evaluated. According to Al-Khattaf,<sup>29</sup> FCC-Y with a unit cell size around 24.5 Å contains only 10% 0-NNN acid sites, whereas the FCC-SY with a unit cell size of 24.27 Å contains approximately 60–70% 0-NNN sites. Hence, FCC-SY catalyst contains a higher amount of strong acid sites (0-NNN), which explains its higher activity for EB disproportionation. Mishin et al.<sup>25</sup> reported that 0-NNN sites play an important role in EB disproportionation over mordenite zeolite. Their results are in good agreement with the present work.

**3.4.4. Coke Yield.** Table 4 reports coke yield for the two catalysts at various reaction conditions. It can be noticed from the table that FCC-Y produces much more coke than catalyst FCC-SY. Although FCC-SY coke yield is in general below 0.1 wt %, FCC-Y coke yield exceeded 2 wt % at 500 °C and 15 s. FCC-Y with large unit cell size favors coking reaction, and these results agree with refs 27 and 28.

## 4. Kinetic Modeling

**4.1 Model Formulation.** Generally, the transformation of EB over zeolites occurs through two main reaction pathways, as shown in the scheme below:



The first reaction pathway, as can be seen above, is *cracking*, which results in the formation of benzene and light hydrocarbons, mainly ethylene. The second reaction pathway, which is *disproportionation*, results in the formation of DEB and benzene. It was observed from the product distribution of EB transformation over FCC-Y catalyst that the transformation occurs mainly through cracking, whereas over FCC-SY the transformation occurs predominantly through disproportionation. Therefore, in modeling the transformation of EB over the FCC-SY catalyst, only the disproportionation reaction pathway was considered. On the basis of this assumption, the following rate equation was written:

Rate of EB disappearance:

$$-r_{EB} = \frac{V}{W_c} \frac{dc_{EB}}{dt} = \eta_e k_d C_{EB} \varphi \quad (4.1)$$

It should be noted that the following assumptions were made in deriving the reaction network: (1) The disproportionation reaction is first order. (2) The model assumes catalytic reactions only and neglects thermal conversion. This hypothesis of a

negligible contribution from thermal reactions has been fully justified.<sup>20</sup> (3) A single deactivation function is defined for all the reactions taking place. (4) The dealkylation reaction is inconsequential due to the minor amounts of gases in the reaction system, especially at low temperature. (5) The reactor operates under isothermal conditions, justified by the negligible temperature change observed during the reactions.

It can be observed from eq 4.1 that the disproportionation reaction is considered to be first-order. This follows a similar assumption made by Nayak and Rieker,<sup>15</sup> Pai et al.,<sup>14</sup> and Das et al.<sup>21</sup> when they modeled the disproportionation of EB. The variable  $c_{EB}$  is the molar concentrations of EB.

$W_c$  is the weight of the catalyst,  $V$  is the volume of the riser simulator, and  $t$  is time. By definition,  $c_{EB}$  is related to the mass fractions of EB,  $y_{EB}$  according to the following equation:

$$c_{EB} = \frac{y_{EB} W_{hc}}{MW_{EB} V} \quad (4.2)$$

where  $W_{hc}$  is the weight of feed (EB) injected into the reactor chamber of the riser simulator and  $MW_{EB}$  is the molecular weight of EB.

The quantity  $\phi$  is the catalyst deactivation function that accounts for catalyst deactivation as the transformation progresses. For the time-on-stream deactivation function employed in this work,  $\phi$  is given by:

$$\varphi = \exp(-\alpha t) \quad (4.3)$$

Where  $\alpha$  is known as the catalyst decay constant.

$\eta_e$  is the effectiveness factor to account for the diffusion constrain on EB. Because of the relative large pore size of the catalyst used and the small size of EB molecule, diffusion constraints may be neglected so that  $\eta_e$  is assumed to be approximately 1.

The activation energy ( $E_D$ ) of the disproportionation reaction is related to the temperature dependent rate constant ( $k_D$ ) according to the Arrhenius equation below,

$$k_D = A_D \exp(-E_D/RT) \quad (4.4)$$

where  $A_D$  is called the pre-exponential factor. To avoid parameter interaction during modeling, Agarwal and Brisk<sup>26</sup> have suggested a reparamatization of eq 4.4 by centering the values of  $k_D$  around  $k_{D0}$  which is the value of the rate constant at the average temperature ( $T_0$ ) of the all the investigated temperatures. Thus,

$$k_D = k_{D0} \exp\left[-\frac{E_D}{R}\left(\frac{1}{T} - \frac{1}{T_0}\right)\right] \quad (4.5)$$

Substituting eqs 4.3–4.5 in eq 4.1, the following differential equations results:

$$\frac{dy_{EB}}{dt} = -k_D G_1 y_{EB} \exp(-\alpha t) \quad (4.6)$$

$G_1$  is the lumped constants given below;

$$G_1 = \frac{W_{hc} W_c}{MW_{EB} V^2}$$

Equation 4.6 contains three important parameters, namely, activation energy ( $E_D$ ) of EB disproportionation, the pre-

(27) Ino, T.; Al-Khattaf, S. *Appl. Catal., A* **1996**, *142*, 5–17.

(28) Pine, L. A.; Maher, P. J.; Wachter, W. A. *J. Catal.* **1984**, *85* (2), 466–476.

(29) Al-Khattaf, S., MS. Dissertation; King Fahd University of Petroleum & Minerals: Dhahran, Saudi Arabia, 1995.

(26) Agarwal, A. K.; Brisk, M. L. *Ind. Eng. Chem. Process Des. Dev.* **1985**, *24*, 203.



exponential constant  $A_D$ , and  $\alpha$ , which is the catalyst decay constant.

**4.2. Model Parameter Determination.** The above-mentioned model parameters were determined by fitting experimental data into eq 4.6 through nonregression analysis using the MATLAB package. Table 5 shows the values of the estimated parameters along with their corresponding 95% confidence limit.

**4.1. Discussion of Kinetic Modeling Results.** The kinetic parameters  $k_{0i}$ ,  $E_i$ , and  $\alpha$ , for the transformation reactions taking place were obtained using nonlinear regression (MATLAB package). Table 5 reports the apparent kinetic parameters along with the corresponding 95% confidence limits for EB conversion using time-on-stream model, the corresponding correlation matrix is presented in Table 5. From the results of the kinetic parameters presented in Table 5, it is observed that catalyst deactivation was found to be very small,  $\alpha = 0.039$ , indicating low coke formation. Disproportionation activation energy of 35.51 kJ/mol was obtained. The correlation matrix (Table 6) displayed low cross-correlation between the regressed parameters, showing that the kinetic parameters are accurate. Pai et al.<sup>14</sup> estimated the activation energy of EB disproportionation over ZSM-5-based catalyst to be 26.27 kJ/mol. On the other hand, Das et al.<sup>21</sup> found the activation energy for the same reaction and in the similar reaction temperature range and over ZSM-5-based catalyst to be 85 kJ/mol. The present activation energy was found to be between these values, although it seems to be closer to the value reported by Pai et al.<sup>14</sup>

To check the validity of the estimated kinetic parameters for use at conditions beyond those of the present study, the fitted parameters were substituted into the comprehensive model developed for this scheme, and the equation was numerically solved using the fourth-order Runge–Kutta routine. The numerical results were compared with the experimental data as shown in Figures 10 and 11. It can be observed from these figures that the calculated results compare well with the experimental data.

## 5. Conclusions

The following conclusions can be drawn from the transformation reaction of EB over the FCC-Y and FCC-SY zeolite catalyst. (1) The results show that EB disproportionation over Y-zeolite-based catalysts is a strong function of acidity and acidity strength. Whereas 0-NNN acid sites favor EB disproportionation, other sites such as 1-, 2-, and 3-NNN promote other reactions such as dealkylation and coke formation. (2) The EB conversion was observed to increase with increase in reaction time and temperature using FCC-SY zeolite. (3) The selectivity

of DEB was highly dependent upon reaction temperature. (4) The molar ratio of benzene/DEB was more than unity, indicating the occurrence of various side reactions. (5) The FCC-Y catalyst, having higher acidity than FCC-SY catalyst, exhibited higher catalytic activity, as reflected in higher values of EB conversions as compared to the FCC-SY. However, selectivity for DEB was very small for FCC-Y catalyst as compared to FCC-SY catalysts. This indicates that, in the case of FCC-Y catalyst, dealkylation and coke formation reactions are dominant over the EB disproportionation reaction. (6) Kinetic parameters for EB disproportionation have been calculated using the catalyst activity decay function based on time-on-stream (TOS).

**Acknowledgment.** The author would like to express his appreciation for King Abdullah University of Science and Technology (KAUST) for their financial support. Also the support of the King Fahd University of Petroleum and Minerals is highly appreciated. Acknowledgement also goes to Mr. Mariano Gica for his help during the experimental work and Dr Nassem Akhter.

## Nomenclature

$C_i$  = concentration of specie  $i$  in the riser simulator (mol/m<sup>3</sup>)

CL = confidence limit

$E_i$  = apparent activation energy of  $i$ th reaction, kJ/mol

$k$  = apparent kinetic rate constant (m<sup>3</sup>/kgcat·s)

$$=k_0 \exp \left[ \frac{-E_R}{R} \left( \frac{1}{T} - \frac{1}{T_0} \right) \right]$$

$k_0$  = pre-exponential factor in Arrhenius equation defined at an average temperature [m<sup>3</sup>/kgcat·s], units based on first-order reaction

$MW_i$  = molecular weight of species  $i$

$r$  = correlation coefficient

$R$  = universal gas constant, kJ/kmol K

$t$  = reaction time (s)

$T$  = reaction temperature, K

$T_0$  = average temperature of the experiment

$V$  = volume of the riser (45 cm<sup>3</sup>)

$W_c$  = mass of the catalysts (0.81 g)

$W_{hc}$  = total mass of hydrocarbons injected in the riser (0.162 g)

$y_i$  = mass fraction of  $i$ th component (wt %)

## Greek Letters

$\alpha$  = apparent deactivation constant, s<sup>-1</sup> (TOS model)

$\eta$  = effectiveness factor

$\varphi_{in}$  = intrinsic decay function

EF8005542